

MeV TOF SIMS analysis of hybrid organic/inorganic compounds in the low energy region

Marko Barac^{1,2}, Marko Brajković¹, Iva Bogdanović Radović¹, Janez Kovač³, Zdravko Siketić^{1,*}

¹Ruđer Bošković Institute, Bijenička c. 54, HR-10000 Zagreb, Croatia

²Jožef Stefan International Postgraduate School, Jamova c. 39, SLO-1000 Ljubljana, Slovenia

³Jožef Stefan Institute, Jamova c. 39, SLO-1000 Ljubljana, Slovenia

*corresponding author, zsiketic@irb.hr

Keywords: low energy MeV SIMS, organic/inorganic compounds, stopping power

This document is the Accepted Manuscript version of a Published Work that appeared in final form in Journal of The American Society for Mass Spectrometry, copyright © American Chemical Society after peer review and technical editing by the publisher. To access the final edited and published work see <https://pubs.acs.org/articlesonrequest/AOR-7MZFNE8WP2BXY7IAIZIW>.

Abstract

The low energy range (a few 100 keV to a few MeV) primary ion mode in MeV Secondary Ion Mass Spectrometry (MeV SIMS) and its potential in exploiting the capabilities of conventional (keV) SIMS and MeV SIMS simultaneously was investigated. The aim is to see if in this energy range both types of materials, inorganic and organic, can be simultaneously analyzed. A feasibility study was conducted, first by analyzing the dependence of secondary ion yields in Indium Tin Oxide (ITO – In₂O₅Sn) and leucine (C₆H₁₃NO₂) on various primary ion energies and charge states of Cu beam, within the scope of equal influence of electronic and nuclear stopping. Expected behavior was observed for both targets (mainly nuclear sputtering for ITO and electronic sputtering for leucine). MeV SIMS images of samples containing separate regions of Cr and leucine were obtained using both keV and MeV primary ions. Based on the image contrast and measured data, the benefit of low energy beam is demonstrated by Cr⁺ intensity leveling with leucine [M+H]⁺ intensity, as opposed to a significant contrast at higher energy. It is estimated that by lowering the energy, leucine [M+H]⁺ yield efficiency lowers roughly 20 times as a price for gaining about 10 times larger efficiency of Cr⁺ yield, while leucine [M+H]⁺ yield still remains sufficiently pronounced.

Address reprint requests to:

Zdravko Siketić, Bijenička c. 54, 10000 Zagreb, Croatia, +38514571227, zsiketic@irb.hr

Introduction

Time-of-flight secondary ion mass spectrometry (TOF SIMS) using primary beam in the MeV energy range has emerged as a promising technique similar to cluster SIMS¹, and has been developed in the recent years in several accelerator facilities around the world. In contrast to the conventional keV SIMS, higher primary ion energies generate significantly higher yields of heavy molecular ions², while causing softer desorption resulting in reduced fragmentation³.

Studies of irradiation effects focus on either displacement damage due to nuclear stopping or the effects of intense electronic excitations and ionization due to a swift heavy ion bombardment of the material. Indeed, in most situations electronic and nuclear stopping are overshadowing one another. Studies that focus specifically on the stopping region where the synergy of electronic and nuclear loss is possibly the most visible are scarce. Recent research⁴ on some clean metallic targets has found that at a significant electronic loss due to swift heavy ion (SHI) bombardment, the majority of the sputtered material is emitted in the neutral state, with only a negligible fraction of ionized particles, which, however, appeared to be larger than under keV bombardment. A significant electronic sputtering effect is observed in some metals, but not in others. Another study⁵ speculated that this could be influenced by a strong electron-phonon coupling and/or a low melting point. The measured yields were not as large as for insulators, but above the predictions for solely nuclear sputtering. Here, the synergy of nuclear and electronic loss was assumed and evaluated using an extended thermal spike model for simulating electronic sputtering by an evaporation process of particles. Experiments on the sputtering of indium atoms under the impact of slow highly charged ions indicated a fundamentally different sputtering mechanism as compared to nuclear sputtering observed under conventional keV primary ion beam⁶. In our most recent study concerning the detection of large organic molecules⁷, an expected increase of the secondary ion yield of phthalocyanine with increasing energy, charge state, electronic stopping, and velocity was found for several different types of primary ions. Although the general trend is valid, there seemed to be no single parameter able to describe the results for all primary ions at once.

In the present study, an idea is introduced to investigate the low energy range (a few 100 keV to a few MeV) primary ion mode in MeV SIMS and its potential benefits in exploiting the capabilities of both conventional (keV) SIMS and MeV SIMS simultaneously – the analysis of samples standardly analyzed by keV SIMS (mostly inorganic species), while still being able to sputter and analyze larger biomolecules. Low energy MeV SIMS may open up a possibility for this fairly new accelerator technique, as well as for other types of instruments, such as ion implanters, to perform mass spectrometry on hybrid organic/inorganic compounds within their technical limits.

Methods

All measurements were performed using 1 MV HVE Tandetron accelerator on the heavy-ion microprobe line at Ruđer Bošković Institute, where the TOF SIMS system is installed⁸. This kind of system is flexible to some degree in terms of primary ion species, energy, and charge state, which is a key advantage in performing these studies. Specifically, the system is limited to a maximal magnetic rigidity equivalent to 8 MeV Si⁴⁺ beam. Measurements were carried out under vacuum (10^{-6} - 10^{-7} hPa). The time-of-flight start signal was defined by a pulsed primary ion beam, achieved with the beam deflector located about 6 meters in front of the sample, and the stop signal was defined by a secondary ion reaching the micro-channel plate (MCP) detector positioned at the end of the linear TOF spectrometer. The voltage applied to the sample holder in order to push the secondary ions into the TOF system was +5 kV, and the MCP detector voltage was set to -2 kV, therefore the instrument was operating in the positive ion mode. The primary ion beam was focused using magnetic quadrupole lenses. All measured secondary ion yields were normalized to the total current that impacted the sample during the measurement. This was done in a way that before and after each measurement, first, direct current was measured in a Faraday cup. Second, the time for which the beam was present on a sample was calculated from the beam deflector geometry, the high voltage switch rise time (10 ns) and the voltage applied to deflect the beam (from 100-500 V), in order to calculate the duty cycle, and thus the effective current that affected the sample. To minimize the effects of sample surface conditions and geometry on the measured secondary molecular yields, spectra were collected from the same sample area. For each measurement, the target angle with respect to the extractor was optimized to maximize the total secondary ion yield. Currents measured on a Faraday cup were ranging from 0.9 – 900 pA, depending on the primary ion species and energy. The beam fluence during all the measurements was kept below the static limit for SIMS⁹ (which is around 10^{12} ions/cm²), so the variation in secondary ion yields due to surface damage can be neglected. Normalized secondary ion yield uncertainties include Faraday cup measured current uncertainties of about 10%, and uncertainties of peak areas (defined by the square root of counts from the linearly fitted background and the square root of counts from net peak area). It should be noted that because of the variations in mass resolution and in the background trends for each energy point, as well as a lack of statistics in certain cases, the uncertainty was sometimes considerable.

In the first part of the study, Indium Tin Oxide (ITO – In₂O₅Sn) and leucine (C₆H₁₃NO₂) were analyzed using Cu primary ions of 7 different energies and charge states, keeping the magnetic rigidity $(m \cdot E)/q^2$ constant for technical simplicity, except for the lowest two energies. Indium ion yield from a 120 nm thick conductive layer of ITO coated on a glass plate, and leucine molecular yields from leucine evaporated on a silicon plate were analyzed.

In the second part, various inorganic species were selected and analyzed using three different primary ion beam energies after Ar⁺ sputter-cleaning of their surfaces.

In the last part of the study, a two-component sample was made in a way that leucine was evaporated partly on Cr, then imaging was performed at the region where both leucine and inorganic part of the sample are present. Measurements were done employing 555 keV Cu^{2+} and 5 MeV Si^{4+} primary ions, with currents ranging from 12 - 20 pA and 200 - 500 pA, respectively. Scan size was around $400 \times 400 \mu\text{m}^2$, with a beam diameter of roughly 50 μm . Furthermore, average spectra of organic and inorganic region were generated. For each primary ion beam, the average pixel spectra were obtained from two clusters generated by k-means clustering algorithm applied on selected principal components after Principal Component Analysis (PCA).

Results and Discussion

Secondary ion yield dependence of In^+ in ITO and main molecular ion in leucine on various primary ion velocities in the low energy MeV SIMS region

In order to investigate the possibility to detect organic molecular ions at low energies and inorganic ions at high energies, as well as to observe general trends in secondary ion yields with respect to the stopping power, ITO and leucine were analyzed using Cu primary ions having 7 different energies and charge states. Primary ion beams used were 150 keV Cu^{2+} , 300 keV Cu^{2+} , 555 keV Cu^{2+} , 1.25 MeV Cu^{3+} , 2.22 MeV Cu^{4+} , 3.47 MeV Cu^{5+} , and 5 MeV Cu^{6+} . Leucine was additionally analyzed using 5 MeV Si^{4+} . The energy/charge state region covered with these beams encompasses the stopping power region in which equal occurrence of nuclear and electronic stopping interaction is expected in each sample. Electronic stopping power was calculated with CasP program¹⁰ (using the UCA model and DHFS screening potential) since it provides non-equilibrium energy loss and considers the charge state of the incident ion. This is crucial in the context of SIMS in which the sputtering occurs from the first few monolayers at the sample surface, where the ion charge state equilibrium is not yet established. Nuclear stopping power was calculated using SRIM¹¹.

Typical MeV SIMS spectra of ITO and leucine obtained with 1.25 MeV Cu^{3+} primary ions are presented in Figure 1. Spectra were normalized to the total number of counts.

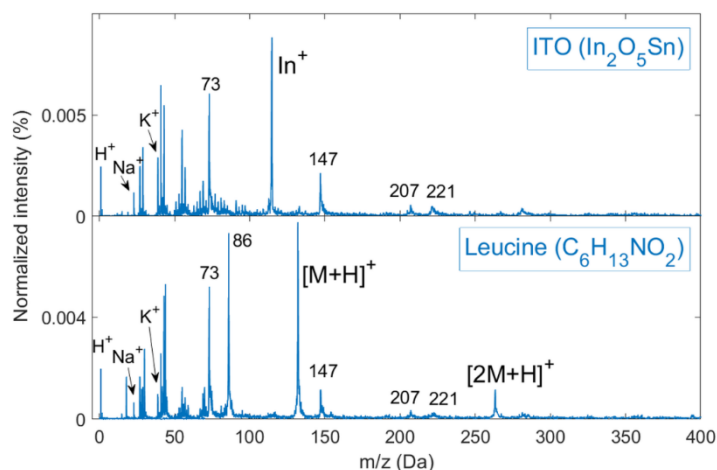


Figure 1. MeV SIMS spectra of ITO and leucine obtained with 1.25 MeV Cu^{3+} primary ions.

Both spectra contain H^+ , Na^+ , and K^+ ions, as well as polydimethylsiloxane (PDMS), which is a usually present contaminant at the sample surface. PDMS characteristic positive ions can be seen at $m/z = 73$ Da, 147 Da, 207 Da and 221 Da, and are often used to calibrate mass spectra. ITO yields In^+ ion at $m/z = 114.8$ Da, which appears to be prominent at this energy. Leucine yields its protonated main molecular ion peak $[\text{M}+\text{H}]^+$ with $m/z = 132$ Da, and $[\text{2M}+\text{H}]^+$ with $m/z = 263$ Da.

Figure 2 shows In^+ secondary ion yield dependence on the primary ion velocity, with respect to the ratio of nuclear and electronic stopping in ITO. The lines in the figure are intended to guide the eye. Clearly, In^+ ions mainly sputter as a consequence of nuclear loss of primary ion energy in the material, since the yield rapidly decreases according to the decrease of nuclear to electronic stopping ratio in ITO. However, the yield starts to slightly increase after around $v/c = 0.009$ (2.22 MeV Cu^{4+}), which indicates the influence of electronic loss on the sputtering of In^+ , as well.

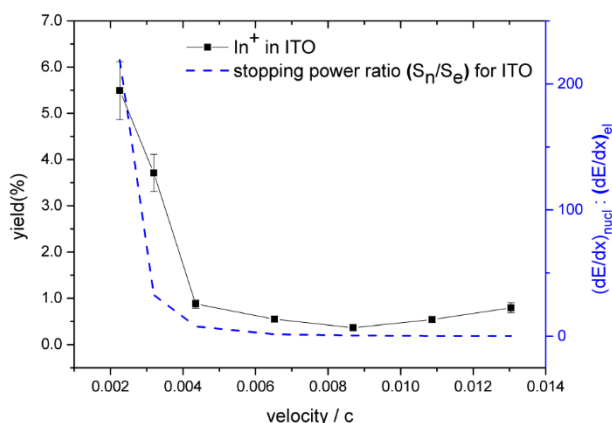


Figure 2. In^+ secondary ion yield dependence on primary ion velocity with respect to the ratio of nuclear and electronic stopping in ITO.

Figure 3 shows leucine protonated main molecular ion yield $[M+H]^+$ with $m/z = 132$ Da, and leucine $m/z = 86$ Da fragment molecular ion yield dependence on primary ion velocity with respect to the ratio of electronic and nuclear stopping in leucine. As an organic compound, leucine is expected to sputter more efficiently on higher energies and charge states. It is clear that the yields of the main molecule and fragment increase in accordance with the electronic loss in leucine. Also, the yield of fragment $m/z = 86$ Da increases more slowly than the main molecular ion yield $[M+H]^+$, which is also expected since it is known that the fragmentation of organic compounds is reduced with increasing electronic loss in the material. This effect is more obvious in Figure 4, where the yield ratio $Y_{86}/Y_{[M+H]^+}$ can be seen decreasing with increasing velocity of the primary ions.

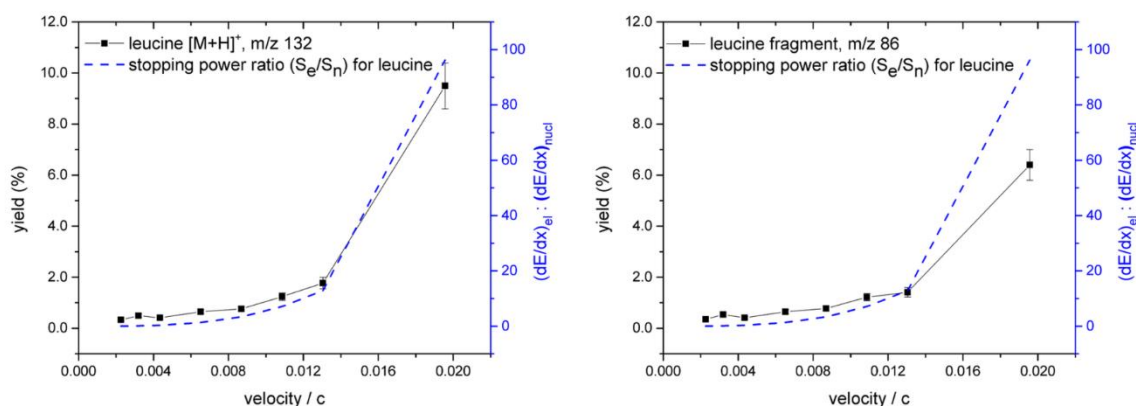


Figure 3. Leucine $m/z = 132$ Da (left) and leucine fragment $m/z = 86$ Da (right) molecular ion yield dependence on primary ion velocity with respect to the ratio of electronic and nuclear stopping in leucine.

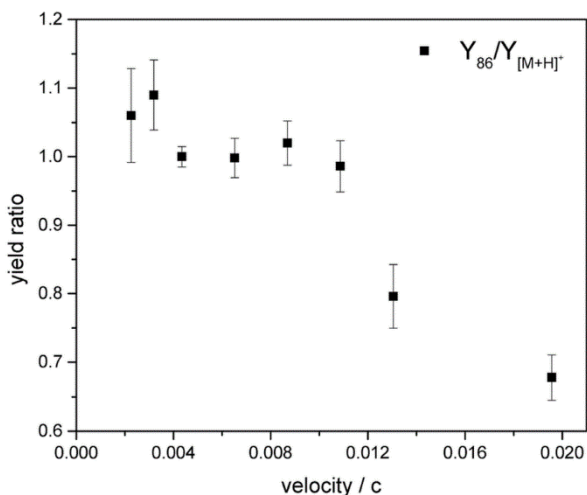


Figure 4. Dependence of yield ratio of leucine fragment $m/z = 86$ Da and main molecular ion $m/z = 132$ Da on primary ion velocity.

Secondary ion yield dependence of selected inorganic species on primary ion velocity

Samples including V, Co, Cr, In, ITO and Sn were all sputter-cleaned before the analysis with 200 keV Cu²⁺, 440 keV Cu²⁺, and 5 MeV Si⁴⁺ primary ions. Sputter-cleaning was performed for 15 minutes with PREVAC Ion Source IS 40C1 operating under E = 3 keV and I = 10 mA, with Ar pressure of about 6 × 10⁻⁶ mbar and current density around 15 μA/cm², which corresponds to Ar⁺ ion fluence of about 8 × 10¹⁶ ions/cm². Secondary ion yields were measured at all three energies and plotted for each sample with respect to the primary ion velocity (Figure 5).

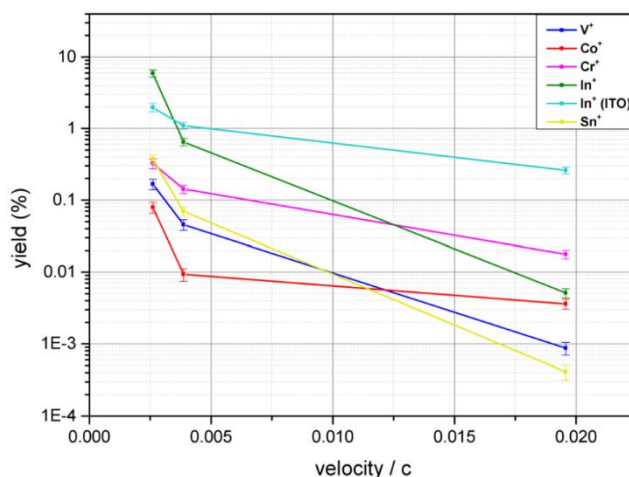


Figure 5. Secondary ion yield dependence of various inorganic ions on primary ion velocity corresponding to 200 keV Cu²⁺, 440 keV Cu²⁺ and 5 MeV Si⁴⁺, respectively.

Clearly, all secondary ions exhibit sputtering behavior influenced mainly by nuclear stopping (which is more pronounced at lower velocities). This is expected for metals because of the considerable dissipation of electronic excitation before any significant energy transfer to the lattice occurs.

Imaging of Cr with partially evaporated leucine with 555 keV Cu²⁺ and 5 MeV Si⁴⁺

In order to investigate the possibility to perform MeV SIMS imaging on a sample consisting of a laterally distributed partly organic and partly inorganic regions and efficiently detect all relevant constituents simultaneously, a target was produced by evaporating leucine powder on a part of Cr foil. Then, imaging was performed at the region where both leucine and Cr area of the sample is present, with 555 keV Cu⁺ and 5 MeV Si⁴⁺ primary ions. It should be noted that the measured area is not precisely the same for 555 keV and 5 MeV primary ions because of the need for beam optimization using Faraday cup after changing the beam. The images are generated by selecting peaks corresponding to Cr⁺ and leucine [M+H]⁺ from the total mass spectrum. Binning by a factor of 2 was applied, resulting in 64x64 pixels, and smoothing with a Gaussian filter (standard deviation of 0.6) in order to flatten random intensity variations across species-specific region. For each primary ion beam energy, Cr⁺ color intensity is normalized to the total leucine [M+H]⁺ yield for comparison. The intensity comparison should be made only between images of different

species obtained with the same primary beam energy, since the data was not normalized to the effective current, but only to the total number of counts.

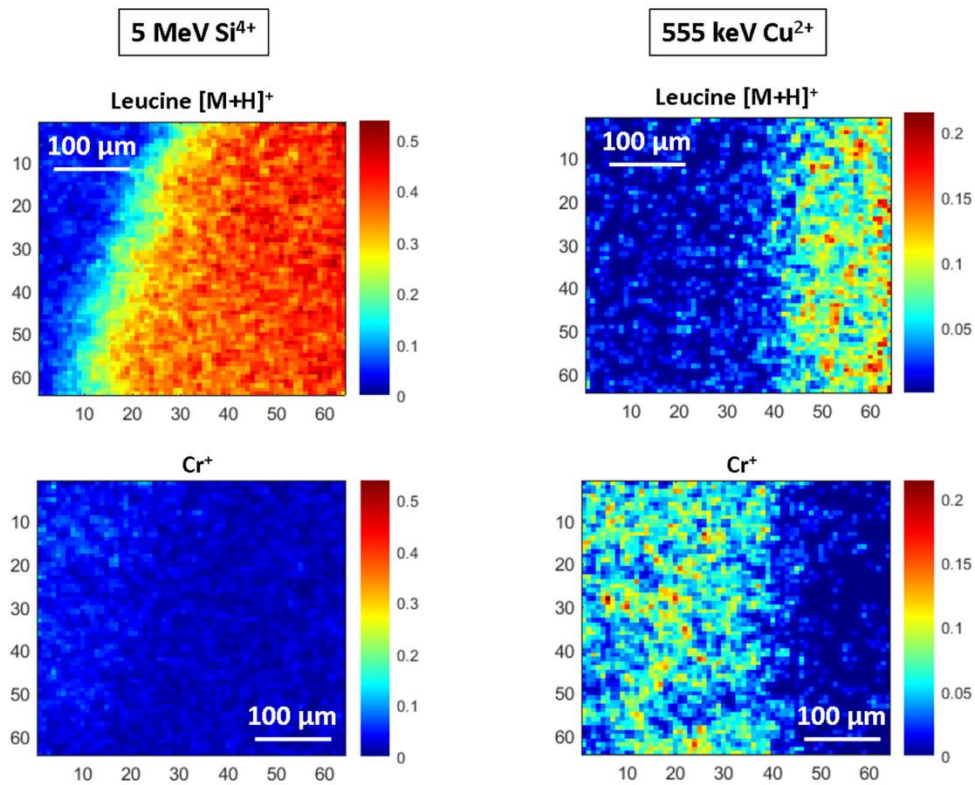


Figure 6. (left) - 5 MeV Si⁴⁺ images of leucine and Cr region. (right) – 555 keV Cu²⁺ images of leucine and Cr region. In each case, Cr⁺ color intensity is normalized to the total leucine [M+H]⁺ yield.

Based on the earlier obtained graphs, one can expect a roughly 20 times higher secondary ion yield of leucine [M+H]⁺ with 5 MeV Si⁴⁺ compared to 555 keV Cu²⁺ primary beam. In contrast, Cr⁺ is expected to be roughly 10 times higher with 555 keV Cu²⁺ versus 5 MeV Si⁴⁺. On the other hand, leucine [M+H]⁺ yield is expected to be around 500 times higher than Cr⁺ yield on 5 MeV Si⁴⁺, and only about twice as high as Cr⁺ on 555 keV Cu²⁺, which is demonstrated in Figure 6. The contrast between leucine [M+H]⁺ and Cr⁺ becomes almost completely diminished by lowering the energy to 555 keV Cu²⁺. In other words, leucine [M+H]⁺ yield efficiency lowers as a price for gaining larger efficiency of Cr⁺ yield, although still remaining pronounced at 555 keV Cu⁺.

The effect can also be observed by comparing spectra of species-particular regions averaged over pixels (Figure 7). Prior to k-means, PCA was applied to the preprocessed data as described in the beginning of this subsection, but the cluster spectra were generated from binned and normalized original image, without smoothing. Cr⁺ peak can be observed from Cr region at 5 MeV Si⁴⁺ in Figure 7.a that is higher than estimated with respect to leucine [M+H]⁺ peak from leucine region, but this could be due to the not well defined interface between two regions as a

result of the beam spot dimension. In Figure 7.b, for 555 keV Cu^{2+} , yields of Cr^+ and leucine $[\text{M}+\text{H}]^+$ become more comparable, with Cr^+ peak showing up.

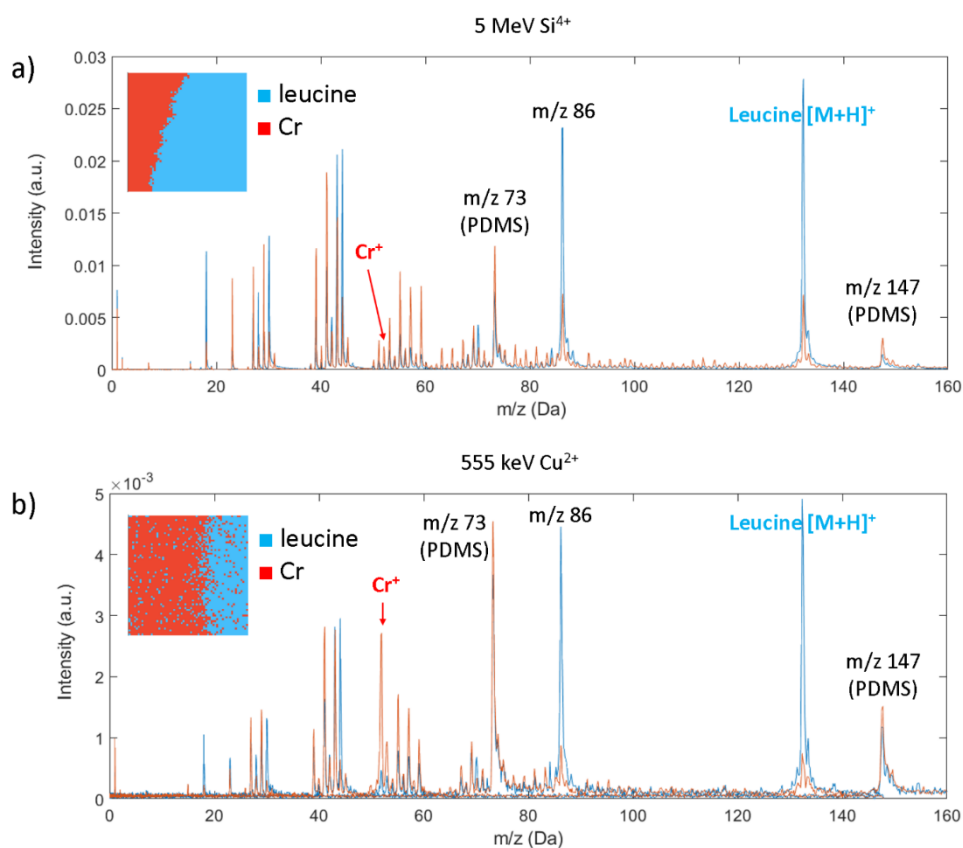


Figure 7. Average cluster spectra of leucine area (blue) and Cr area (red) from MeV SIMS image obtained with a) 5 MeV Si^{4+} and b) 555 keV Cu^{2+} .

Conclusions

In the present study, the expected behavior of the secondary ion yield of In^+ in ITO, and the main molecular ion $[\text{M}+\text{H}]^+$ from leucine is observed with regard to the nuclear and electronic energy loss in the material, respectively. It was found that in the stopping region covered with the used primary ion beams, a synergy of electronic and nuclear loss could occur, but this depends mainly on the sample characteristics. Nevertheless, the observed trends in the secondary ion yields mostly show the dominance of either nuclear (ITO) or electronic (leucine) stopping, yet with indications of electronic stopping influence on In^+ yield in ITO at higher velocities. Also, the molecular ion yield of leucine fragment at $m/z = 86$ Da expressed the anticipated behavior – the yield increases with the electronic stopping, while the ratio of the fragment ion and the main molecular ion yield decreases, indicating that the fragmentation is reduced for higher primary ion velocities.

Selected inorganic species were successfully detected at all three primary ion beam energies, exhibiting expected behavior of secondary ion yield with respect to the primary ion velocity –

yields decreasing with increasing velocity, i.e. decreasing nuclear stopping in the inorganic material, which is a driving force in collisional sputtering.

MeV SIMS images were obtained using 555 keV Cu²⁺ and 5 MeV Si⁴⁺ primary ions on a hybrid sample consisting of regions containing Cr and leucine, laterally separated. It is anticipated that lowering the energy to 555 keV Cu²⁺, leucine [M+H]⁺ yield efficiency is reduced roughly 20 times as a price for gaining about 10 times higher efficiency of Cr⁺ yield, while still remaining prominent at low energy. Based on the results from this study, it can be concluded that there is a potential for imaging of hybrid organic/inorganic samples with ions in the energy range where electronic and nuclear stopping power contribute almost equally.

Acknowledgments

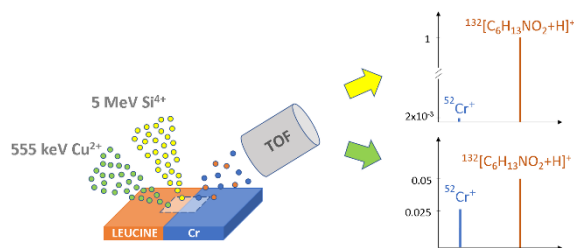
Authors acknowledge support by the RADIATE project under the Grant Agreement 824096 from the EU Research and Innovation program HORIZON 2020 and by the Croatian Centre of Excellence for Advanced Materials and Sensing devices research unit Ion Beam Physics and Technology, Ruđer Bošković Institute, Zagreb, Croatia. M. Brajković acknowledges support by the Croatian Science Foundation (CSF) project "Young Researchers' Career Development Project - Training of Doctoral Students" co-financed by the European Union, Operational Program "Efficient Human Resources 2014-2020".

References

1. Jones, B. N.; Matsuo, J.; Nakata, Y.; Yamada, H.; Watts, J.; Hinder, S.; Palitsin, V.; Webb, R., Comparison of MeV monomer ion and keV cluster ToF-SIMS. *Surface and Interface Analysis* **2010**, *43* (1-2), 249-252.
2. Nakata, Y.; Honda, Y.; Ninomiya, S.; Seki, T.; Aoki, T.; Matsuo, J., Yield enhancement of molecular ions with MeV ion-induced electronic excitation. *Applied Surface Science* **2008**, *255* (4), 1591-1594.
3. Kamensky, I.; Håkansson, P.; Sundqvist, B.; McNeal, C. J.; Macfarlane, R., Comparison of biomolecule desorption yields for low and high energy primary ions. *Nuclear Instruments and Methods in Physics Research* **1982**, *198* (1), 65-68.
4. Breuer, L.; Ernst, P.; Herder, M.; Meinerzhagen, F.; Bender, M.; Severin, D.; Wucher, A., Mass spectrometric investigation of material sputtered under swift heavy ion bombardment. *Nuclear Instruments and Methods in Physics Research Section B: Beam Interactions with Materials and Atoms* **2018**, *435*, 101-110.
5. Mieskes, H. D.; Assmann, W.; Grüner, F.; Kucal, H.; Wang, Z. G.; Toulemonde, M., Electronic and nuclear thermal spike effects in sputtering of metals with energetic heavy ions. *Physical Review B* **2003**, *67* (15).

6. Herder, M.; Ernst, P.; Skopinski, L.; Weidtmann, B.; Schleberger, M.; Wucher, A., Ionization probability of sputtered indium atoms under impact of slow highly charged ions. *Journal of Vacuum Science & Technology B* **2020**, *38* (4), 044003.
7. Brajković, M.; Barac, M.; Bogdanović Radović, I.; Siketić, Z., Dependence of Megaelectron Volt Time-of-Flight Secondary Ion Mass Spectrometry Secondary Molecular Ion Yield from Phthalocyanine Blue on Primary Ion Stopping Power. *Journal of the American Society for Mass Spectrometry* **2020**, *31* (7), 1518-1524.
8. Tadić, T.; Bogdanović Radović, I.; Siketić, Z.; Cosic, D. D.; Skukan, N.; Jakšić, M.; Matsuo, J., Development of a TOF SIMS setup at the Zagreb heavy ion microbeam facility. *Nuclear Instruments and Methods in Physics Research Section B: Beam Interactions with Materials and Atoms* **2014**, *332*, 234-237.
9. Amstalden van Hove, E. R.; Smith, D. F.; Heeren, R. M. A., A concise review of mass spectrometry imaging. *Journal of Chromatography A* **2010**, *1217* (25), 3946-3954.
10. Grande, P. L.; Schiwietz, G., The unitary convolution approximation for heavy ions. *Nuclear Instruments and Methods in Physics Research Section B: Beam Interactions with Materials and Atoms* **2002**, *195* (1-2), 55-63.
11. Ziegler, J. F.; Ziegler, M. D.; Biersack, J. P., SRIM – The stopping and range of ions in matter (2010). *Nuclear Instruments and Methods in Physics Research Section B: Beam Interactions with Materials and Atoms* **2010**, *268* (11-12), 1818-1823.

For Table of Contents Only:



Manuscript title: MeV TOF SIMS analysis of hybrid organic/inorganic compounds in the low energy region - a feasibility study

Authors: Marko Barac, Marko Brajković, Zdravko Siketić, Iva Bogdanović Radović, Janez Kovač

Description of graphic: MeV TOF SIMS spectra obtained with 5 MeV Si⁴⁺ and 555 keV Cu²⁺ on a hybrid leucine/Cr sample. Lowering the energy to unconventional 555 keV, the secondary ion yield of Cr⁺ is expected to rise compared to a decrease in leucine main molecular ion yield, resulting in a more leveled and comparable yields.